

A Numerical Model to Investigate the Role of Residual Stresses on the Mechanical Behavior of Al/Al_2O_3 Particulate Composites

M. Guagliano

(Submitted 15 August 1997; in revised form 14 October 1997)

Research is presented about the mechanical behavior of a 6061 aluminum alloy reinforced with alumina particles. In particular, the role of thermal-induced residual stresses on the mechanical behavior of this composite is analyzed. Experimental tests were carried out to evaluate the mechanical characteristics of this type of material under static and fatigue loading. Fractographies on broken specimens evidenced the failure mechanisms under different load conditions. Also carried out were measurements using the x-ray diffractometric (XRD) technique to determine the residual stresses due to the thermal treatment both in the matrix and in the particles. A microscale finite-element model (FEM) of this material was developed to investigate the actual stress state caused by the thermal treatment and an applied load. A comparison of the numerical results and the experimental observations helped to explain the fracture modes under static and cyclic loading and to determine the role of the residual stresses under both monotone and cyclic loads. These results suggest some treatment to improve fatigue strength of the material.

Keywords FEM, MMCs, residual stress, XRD

1. Introduction

Due to their good strength-to-weight ratio, metal matrix composites have been increasingly used in various engineering fields. In particular, aluminum matrix composites have been used in aircraft for many years and more recently in automotive components, cross-country bicycles, and other sports equipment (Ref 1). However, to exploit these materials, it is essential to be fully aware of their mechanical characteristics. Not only is it important to understand the mechanical behavior of these types of materials, but it is also necessary to determine the location a fracture might occur (in the matrix, in the particles, or at the interface).

From a mechanical viewpoint, it is necessary to know the strength of materials in the composite and the local stress/strain response in the different parts of the material under an applied load. Complete characterization of the mechanical behavior of the material requires a determination of the residual stress state induced by thermal treatment and its influence on mechanical properties. Hence, different approaches can be found.

Eshelby (Ref 2) solved the elastic problem of an isolated ellipsoidal inhomogeneity embedded in an infinite domain under the action of a uniform remote stress field. Eshelby's approach led to the development of a theoretical model capable of predicting the average residual stresses induced in the matrix by the cool-down process (Ref 3).

The recent ever-increasing development of the finite-element method (FEM) has aided in the development of numerical models representing microstructural schemes of different kinds of composite materials. This type of approach is advantageous in that shapes similar to those experimentally observed can be modeled and analyzed. Furthermore, the elastoplastic behavior of the matrix and, consequently, phenomena such as the Baushinger effect and work hardening due to plastic deformation are taken into account. The latter mentioned method provides an accurate account of the stresses and strains throughout a specific time history, for example, during a heat treatment.

Finite element models can be two-dimensional or three-dimensional. Generally, three-dimensional models lead to a better description of the stress-strain state in the material. However to obtain reliable results, the models must be quite accurate, which can be costly. Furthermore, these models require powerful computers. If the studied models are coarse, the results obtained cannot be considered reliable especially if the mechanical behavior of the matrix-reinforcement interface is considered. In fact, this problem involves a nonlinearity due to the contact of the two phases and the nonlinear behavior of the material. These factors contribute to considerable numerical difficulties and calculation time.

Yet two-dimensional FEMs may give useful information about the mechanical behavior of the composite without necessitating expensive computer facilities. Levy and Papazian (Ref 4) developed two three-dimensional models of a SiC/Al composite material. The reinforcements were assumed to be cylindrical and aligned in a three-dimensional array. Levy and Papazian (Ref 4) analyzed the influence of the relative position of particles which were transversely aligned or staggered. The elastoplastic nature of the matrix were considered whereas, the properties of the interface were not considered. Further analysis of their model allowed Levy and Papazian (Ref 5) to also take into account the effect of the residual stresses caused by heat treatment.

Xu and Watt (Ref 6) used the FEM to study the role of a hard particle in a metal matrix. Their analysis was based on the re-

M. Guagliano, Dip. to Meccanica, Politecnico di Milano, P.zza L. da Vinci, 32, 20133 Milano, Italy.

sults obtained by Eshelby (Ref 2), but the effect of the interface was not considered.

On the contrary, the model developed by Wisnom (Ref 7) considers the role of the interface using special finite elements, although the interface strength had to be assumed arbitrarily. Sadouki and Wittmann (Ref 8) developed a general model that simulated the presence of an interface with springs and damping elements. Christman et al. (Ref 9) studied the influence of factors such as shape, distribution, volume fraction, and clustering, on the mechanical behavior of a reinforced 2014Al alloy.

More recently, Ho and Saigal (Ref 10) calculated the residual stresses resulting from thermal treatment and evaluated their effect on the tensile curve and strength. They used a three-dimensional FEM to simulate the changes of material characteristics because of the heat treatment. Conversely, Llorca and Poza (Ref 11) developed a numerical model to investigate the cyclic behavior of a ceramic-reinforced aluminum alloy.

The commonality of all these models is that they use silicon carbide particles for reinforcement. However, due to the particle shape, the nature of the interface, and the mechanical behavior of the metal matrix, the modeling scheme of these composites cannot be generalized.

In this article, an Al/Al_2O_3 composite was considered. Because experimental observations showed that the alumina particle cannot be compared to a cylinder or a spherical inclusion an appropriate numerical microscale model of the studied material was developed to investigate the effects of thermal treatment in terms of induced residual stresses and to understand the actual stress-state both in the matrix and in the particle under tensile load action. The interface was simulated by a numerical technique capable of reproducing the specific nature of the contact between alumina and aluminum. The role of the residual stresses deriving from the thermal treatment and from the applied loads was analyzed and compared with residual stresses measured using the XRD technique.

The results were validated by comparing them with the tensile stress-strain curve. They also were compared with the results obtained in tensile and fatigue tests. These results then were used to interpret the failure modes and mechanisms observed to subsequently explain the actual behavior of the material and to illustrate the role played by residual stresses on mechanical properties.

Table 1 Physical and mechanical characteristics of 6061 aluminum alloy and Al_2O_3

Property	6061 Al	Al_2O_3
Elastic modulus, MPa		297000
At 293 K	69000	
At 373 K	68000	
At 423 K	66000	
At 473 K	61000	
At 523 K	55000	
At 573 K	45000	
Poisson ratio	0.33	0.21
Yield stress, $R_{p0.2}$, MPa		
At 293 K	276	
At 373 K	262	
At 423 K	248	
At 473 K	221	
At 523 K	165	
At 573 K	90	
Ultimate tensile strength, R_m, MPa		
At 293 K	310	
At 373 K	283	
At 423 K	262	
At 473 K	228	
At 523 K	172	
At 573 K	97	
Elongation, %	17	
Density, kg/m^3	2700	3720
Thermal conductivity, W/m·K	167	19
Coefficient of thermal expansion, 1E-06K^{-1}	23.6	7.4

Table 2 Mechanical characteristics of 6061 Al/Al_2O_3 composite material

Characteristic	Value
Elastic modulus, E, MPa	92800 ± 1000
Poisson ratio	0.31 ± 0.02
Ultimate tensile strength, MPa	370 ± 5
Yield stress, MPa	342 ± 10
Elongation, %	4 ± 1.5

2. Material and Experimental Tests

The composite material tested was W6A20A, which is manufactured by DURALCAN, USA. It consists of an aluminum 6061 alloy matrix, and the reinforcement is made of Al_2O_3 particles with an average size of about 15 to 20 μm. An average dimension ratio of 2 was observed, and a volume fraction was 20%. The mechanical characteristics of the matrix and of the reinforcements are illustrated as a function of temperature in Table 1 (Ref 12).

The material was solutionized for 2 h at 530 °C, water quenched, and then aged for 15 h at 165 °C (this treatment is usually called T6). Tensile tests were carried out on cylindrical specimens according to ASTM E 8-95 standards. The average results obtained from five tests performed at room temperature are shown in Table 2.

Rotating bending fatigue tests on smooth specimens were performed to evaluate the behavior of this material under cyclic loading and to analyze the failure mechanisms at different stress levels. Detailed fatigue test results are found in Ref 13.

Surface residual stresses due to the heat treatment were measured using an XRD. Table 3 shows the details of the x-ray

Table 3 Detail of x-ray measurement conditions

Equipment:
Target, Cr Rigaku Strainflex
Filter, V Rigaku Strainflex

Diffraction planes:
Aluminum, (311)
Irradiated area, 1 × 1 mm^2
Incident angles, 0, 15, 25, 35, 45
Geometry, side inclination
Method, $\sin^2\psi$

measurements. Fractographies on the fracture surfaces of the broken specimens completed the experimental analysis.

3. Finite-Element Analyses

A two-dimensional and plane-strain model of the microstructure of the composite was developed to investigate the role of residual stresses on the actual mechanical behavior of the composite material. The finite element code used is ABAQUS.

The three-dimensional nature of the problem was neglected because of the shape of the reinforcement particles and the numerical difficulties due to the simulation of the contact between the particle and the matrix. This made it impossible to build a three-dimensional mesh fine enough to reproduce the stress-strain state correctly.

The model is based on a cell of an alumina particle surrounded by the matrix. Particles were equal to 18 μm long and 9 μm wide, resulting in a dimensional ratio of 1:2, which was similar to the one observed experimentally. Spacing between particles was 11 μm in direction 1 and 5.5 μm in direction 2 (Fig. 3) so that in the plane model the actual 1:5 volume ratio was maintained. Because the model is made of plane-strain elements, this assumption can appear incorrect; however, in this model, the thickness of the matrix and the particle is the same, but the local stress-strain response will be affected by this assumption.

This basic cell is repeated to simulate the presence of a set of aligned particles. Other ordered particle layouts were not considered because recent technological improvements made it possible to align the particles satisfactorily in any direction and because Levy and Papazian (Ref 4) found that the most realistic layout is the one considered in the present analysis.

Basing the analysis on many microscopical observations, the shape of the alumina particle was octagonal and stretched in one direction. The experimental investigations showed that the particles did not have sharp corners, unlike the SiC particles commonly found in this type of analysis. Figure 1 shows the mesh of the material compared to an experimental particle. A nine-particle model was developed and used to carry out analyses with different boundary conditions. Nevertheless, the most interesting results obtained were those presented with symmetrical boundary conditions and applied loads. Yet the boundary nodes of the model were restrained by symmetrical boundary conditions, thus simulating the action of surrounding material.

Another important consideration is correct simulation of the mechanical behavior of the interface between particles and matrix. In fact, this type of composite is characterized by the presence of spinel crystals at the interface. These crystals prevent the macrosliding of the two components and their separation, until the material breaks. Special elements were used, allowing for normal contact and sliding. The Lagrange multiplier contact approach (Ref 14, 15) was used to numerically schematize the particular behavior of the spinel crystals. This does not provide any slip, but facilitates contact surface separation. Other analyses have been carried out by using the classical Coulomb contact theory and by varying the friction coefficient, to investigate the quantitative influence of the numerical characteristic of the interface.

The material behavior of the matrix was simulated by reproducing the experimental trend of the tensile curve while the alumina was schematized as a perfectly linear material.

Another peculiarity of this model is that the thermal and the mechanical analyses are conducted at different times using different, but interdependent, models. The advantage of this procedure is that the analyses can be optimized. In fact, the analyses are performed in the time domain, and at successive increments. By separating the thermal and the mechanical analyses, it is possible to choose the best increments for each analysis, which do not necessarily have to be the same increments.

For both calculations, the mesh must be the same even though the type of element changes. In the first analysis, the

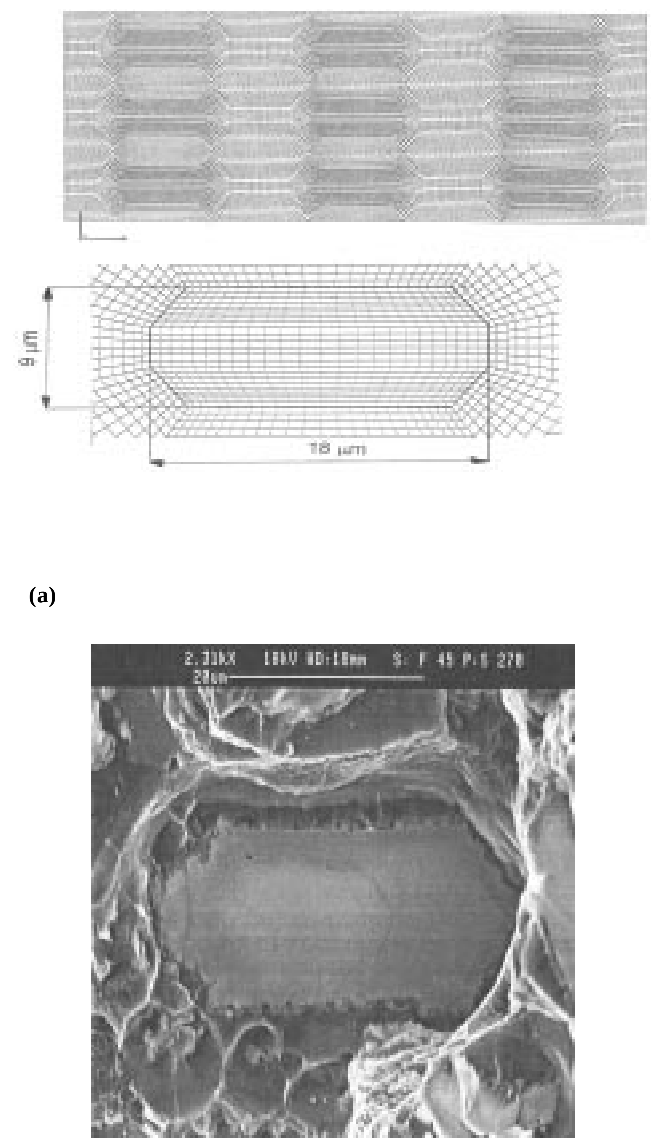

(a)

(b)

Fig. 1 (a) Mesh of the composite material, particular of the particle. (b) Alumina particle observed via electronic microscope thermal transient caused by the heat treatment is simulated, and the temperature distribution is calculated.

The thermal law imposed on the boundary of the model simulates cooling of the water from 573 to 293 K. For temperatures higher than 573 K, the material is assumed to be free residual stresses. The material is then heated to 438 K, and the artificial aging is simulated. To make the heat transfer from the matrix to the alumina particle possible, the particular one-dimensional elements between opposite nodes of the matrix and the particle were constructed. This heat conduction simulation at the interface can be compared with the presence of the spinel crystals, which in some way influence the uniform heat diffusion in that area. The values of the heat transfer coefficients of these elements were taken as the average values of the matrix and particles. The numerical procedure allowed simulation of the heat transfer between the matrix and water or air. This simulation was possible by a boundary surface and calculation of the convective heat transfer coefficient *h* for water and air, where the heat treatment is made. The *h* value was determined using the procedure described in Ref 10 using the dimensionless Rayleigh (Ra) and Nusselt (Nu) numbers.

In the mechanical analysis, the stresses were derived from the temperature distribution calculated in the thermal transient. The transformation of the mechanical characteristics during the thermal transient was followed by assigning the values in Table 1. At the end of the analysis, a tensile load was applied, and the actual stress-strain state in the material model was calculated.

4. Results and Discussion

Different preliminary analyses were made of the thermal treatment by considering one particle (free to move at the boundaries), by using the Coulomb contact law and by chang-

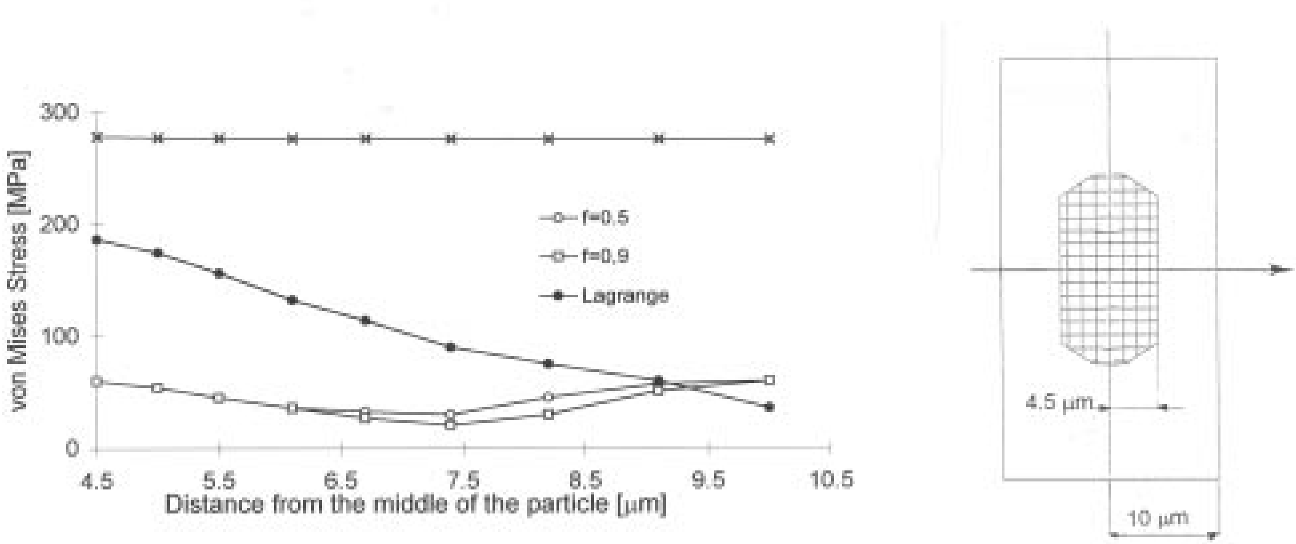

Fig. 2 Von Mises equivalent stress trend for the different interface simulations tested (thermal treatment analyses)

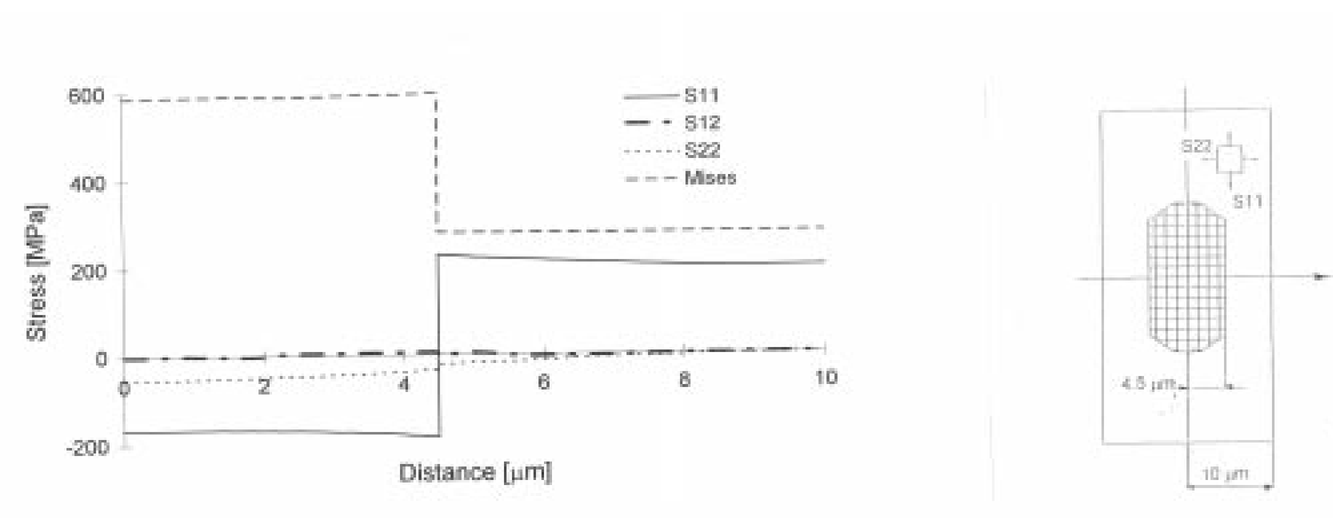

Fig. 3 Trend of the different stress components in the middle section of the center particle (thermal treatment analysis)

ing the friction coefficient. Results were compared with those obtained using the Lagrange multiplier contact approach. The aim being to evidence the importance of the contact algorithm chosen. This comparison shows that similar trends are obtained by using the Coulomb contact approach with different friction coefficients. A different trend is obtained using the Lagrange multiplier approach. In particular, the von Mises equivalent stress, defined as:

$$\sqrt{S_I{}^2 + S_{II}{}^2 + S_{III}{}^2 - S_I S_{II} - S_{II} S_{III} - S_I S_{III}}$$

where S_I, S_{II}, and S_{III} are the principal stresses. These increase near the interface due to the shear stresses that arise, particularly near the corners, to prevent sliding.

Figure 2 shows the trend for the different models tested in terms of the von Mises equivalent stress: the results of the nine particles (free to move at boundaries of the model) refer to the central one. The difference between the trends of one and nine particles is due to the boundary conditions and shows the importance of the correct choice of the kinematic conditions at the boundaries. Considering the physical nature of the interface (which prevents macrosliding), the Lagrange multiplier approach was chosen for the final nine-particle model. Different analyses were conducted on this model, simulating the thermal treatment, monotonically increasing the load, and a cyclic repetition of load.

4.1 Thermal Treatment

The boundary conditions imposed along the edges are those of double symmetry to simulate the internal layers of materials. Figure 3 illustrates the trend of the stress components $S_{11}$and S_{22} along the matrix and the central particle (directions 1 and 2 are shown in Fig. 3). Note that in the section considered, the matrix is subjected to tensile residual stresses along direction 1. The residual shear stresses are not large, and during thermal treatment, the formation of spinel crystals is not involved in the prevention of sliding and in the development of a detrimental residual stress state. This is mainly due to the different thermal expansion coefficients of the matrix and the particles.

If the von Mises residual stress trend is compared with that obtained by considering only one particle without kinematic restraint at the boundaries, the strong influence that the interaction with the other particles has on the residual stress state is evident. The value in the matrix, in the proximity of the interface, doubles.

The numerical results were compared with the experimental residual stress measurements obtained using an XRD. The residual stress state in the matrix, soon after the thermal treatment and before any other mechanical working, proved to be about equibiaxial, and the average value of ten measurements was 50 ± 5 MPa. Because of the area affected by the x-ray beam (1 mm^2), the obtained values can be considered as average values of the actual trend. Consequently, comparison with the numerical results may be considered satisfactory and supported by the fact that if these analyses are enlarged to cover a larger area around the particle, then there are zones that were not affected by residual stresses or that preset small values of residual stresses. Therefore, the average value on a finite area of measurement reduces with respect to the trend shown in Fig. 3.

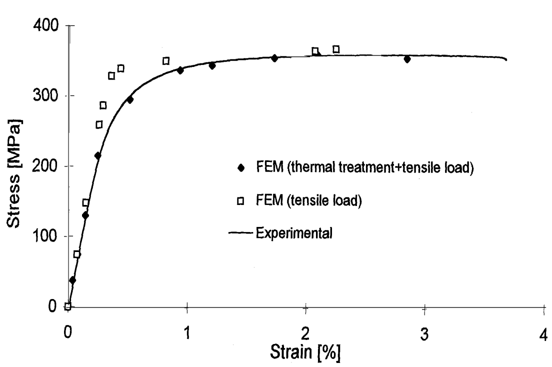

Fig. 4 Tensile stress-strain curves obtained numerically and experimentally

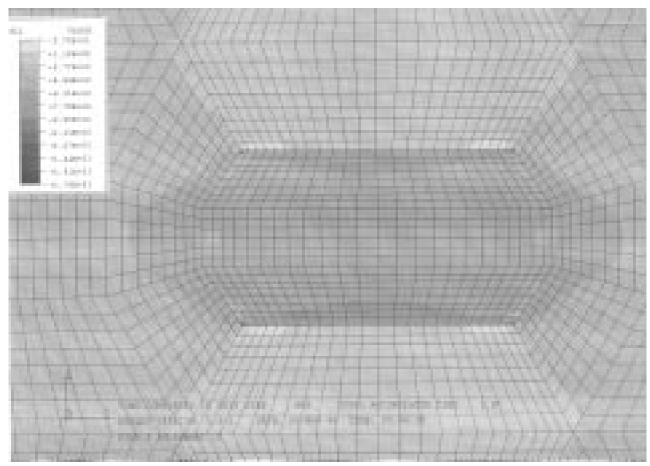

(a)

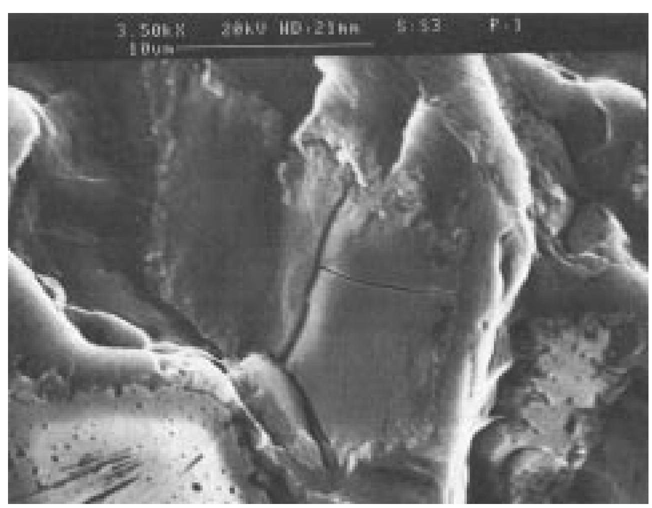

(b)

Fig. 5 (a) Stress in direction 1 ($S11$) contours around and in the reinforcement particle. (b) SEM image of the fracture surface (thermal treatment and monotonic applied load)

4.2 Monotonic Applied Load

The second analysis involves the mechanical behavior of the composite material following a thermal treatment and implies a tensile load applied along direction 1. Figure 4 shows

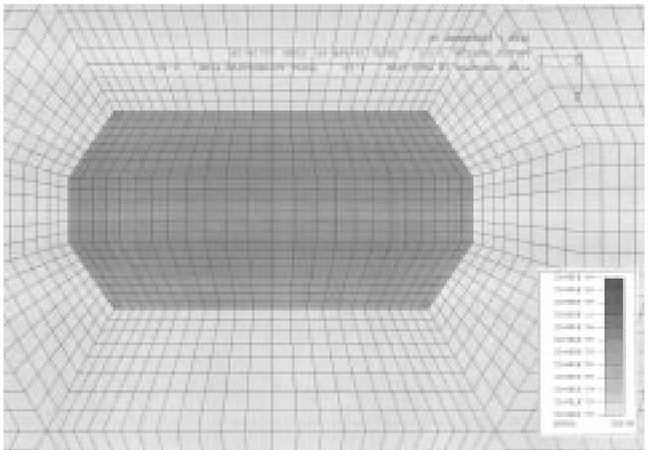

Fig. 6 Von Mises equivalent stress contours in and around the reinforcement particle (thermal treatment and monotonic applied load)

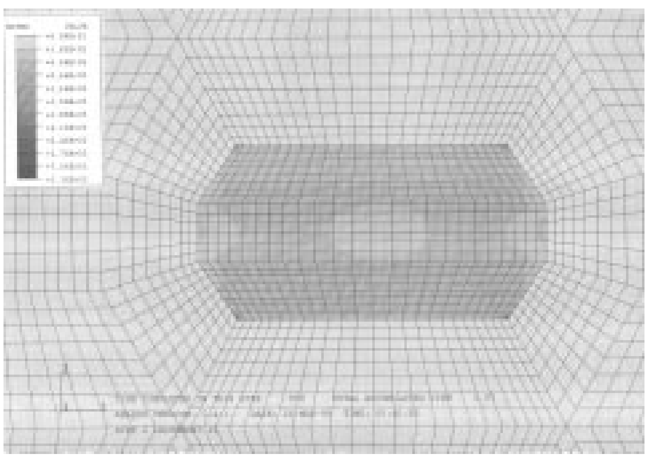

(a)

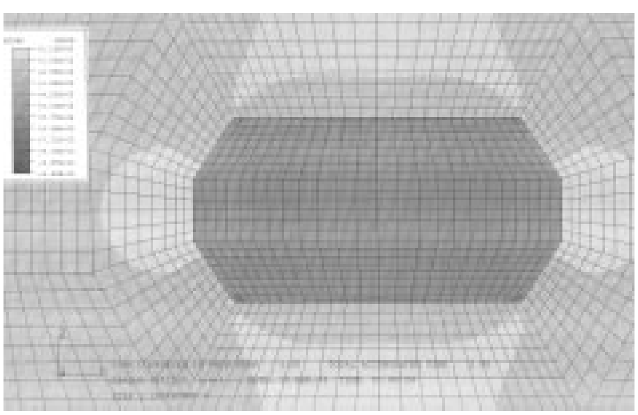

(b)

Fig. 7 Von Mises equivalent stress (a) after the thermal treatment and (b) after the load cycle

the comparison between the stress-strain curve obtained experimentally and numerically. Agreement is good until the highest load is applied, which can be considered as validation of the FEM microstructure model. Figure 4 also shows the role played by the residual stresses by the curve obtained without taking the thermal treatment into account. In fact, the numerical stress-strain curve obtained by considering the thermal treatment is approximate to the experimental one, both in the elastic and the elastoplastic fields. The global elastic modulus is practically equal to the experimental modulus (E_{exp} = 92.800 MPa, E_{FEM} = 93 200 MPa), whereas the value numerically obtained without considering the thermal treatment is 10% higher (E_{FEM} = 101.800 MPa, without residual stresses). This can be attributed to local plasticization of the matrix near the sharp corners at the interface with the reinforcement. Due to the presence of residual stresses, this occurs for low applied loads and globally reduces the elastic modulus. Furthermore, the presence of the tensile residual stresses in the matrix causes yields for low loads. This also is in concordance with the experimental evidence.

Figure 5(a) shows the longitudinal stress (S_{11}) map across and over the particle. The most stressed zone is in the middle of the particle. This agrees with experimental observations. In fact, scanning electron microscopy (SEM) observations show that there are many particles broken in the middle section of the fracture surface (Fig. 5b).

On the contrary, the matrix is subjected to low stresses. Figure 6 shows the von Mises stress around the particle where the trend is uniform and lower than the yield stress.

4.3 Cyclic Loading

Further analyses assessed the mechanical behavior of the composite in alternate cyclic loading where the cyclic loading was equal to the fatigue limit of the material (160 MPa). According to Ref 11, and due to the lack of reference experimental data, the matrix was assumed to harden isotropically.

In this case too, two types of analyses were carried out. The first analysis did not consider the thermal treatment while the second considered the effects of the thermal treatment. The

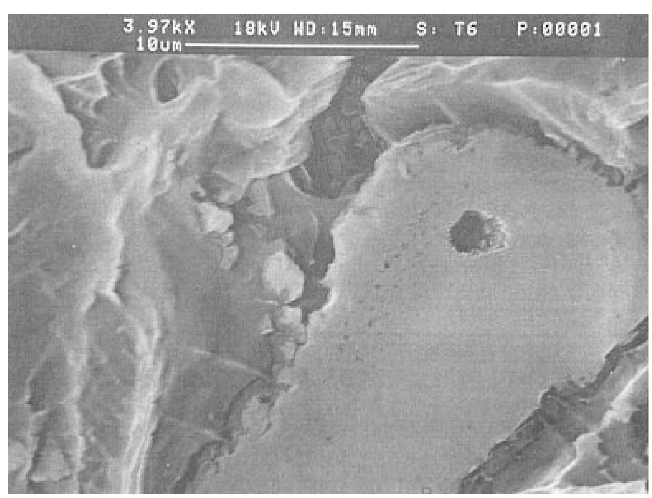

Fig. 8 SEM image of the decohesion between matrix and particle

first analysis showed that the global stress state throughout the material does not reach near the yield stress values. The reinforcement particle is not subjected to dangerous stresses.

If residual stresses caused by thermal treatment in the matrix are observed, the von Mises stress is locally higher than the yield stress inducing plasticization. Figure 7 shows the initial stress distribution (Fig. 7a) and the stabilized residual stress situation (Fig. 7b). Figure 7 demonstrates that the residual stress concentration on the boundary of the particle, after the application of the load cycle, did not change. Whereas at distances away from the reinforcement, the residual stresses remain similar to the initial stresses, and the fatigue damage process is able to be interpreted.

In fact, the repeated application of the load causes damage to the interface (fracture of the spinel crystals or decohesion of the particle and the matrix) or the formation of voids in the matrix, thus resulting in fatigue crack initiation. This agrees with the experimental observations of fatigue-broken specimens, in which it is possible to note decohesion and a lack of sliding between the matrix and the particle (see Fig. 8). Also, the presence of thermal-induced residual stresses appears to strongly influence the behavior of the material. In particular, the tensile stresses present in the matrix limit the increment of the fatigue limit with respect to the nonreinforced alloy.

5. Conclusions

The investigation of the mechanical behavior of a particle-reinforced metal matrix material by means of numerical analyses and experimental observations led to the following conclusions.

A finite-element model simulating the microstructure of a Al/Al_2O_3 composite material was developed. The model shows original aspects in respect to those present in the literature. In fact, the shape of the particle reproduces the geometry of the alumina particles better than the cylindrical particles. The interface was simulated using a special algorithm, which although it prevents macrosliding, allows for surface separation and consequently reproduces the behavior of the interface formed by spinel crystals. The present model is quite general, well-verified in terms of the global behavior of the material. A comparison of it with the experimental tensile stress-strain curve can be used to simulate different kinds of materials by changing the ratio between the volume of the particles and the matrix.

The thermal treatment of the composite was simulated to determine the residual stress pattern induced. The obtained values, the average of which seems to agree with the experimental measurements, show high stress concentrations near the corners of the particles.

Numerical analyses, which were carried out with the application of a tensile load, show the critical point to be in the middle of the particle. Due to the local plasticization near the interface, the thermal-induced residual stresses minimally affect the elastic modulus and the yield stress of the material. Comparison of the results obtained by applying a tensile load, with and without the heat treatment, evidenced the importance of residual stresses on the behavior of the material under static loads.

Thermal-induced residual stresses also play an important role in the high-cycle fatigue region. In fact, without their presence, the stress state near the interface would not reach a critical value. Furthermore, residual stresses are the main cause of the interface damage and, consequently, of the fatigue crack initiation.

The quantitative values of the stress cited above are influenced by the plane schematization of the material. However, the simplified model which was developed provides useful information about the damage mechanism under both monotonic and cyclic loading.

The results suggest that, in order to improve fatigue behavior of this type of material, it is necessary to perform a surface treatment capable of inducing compressive residual stresses and preventing fatigue crack propagation in its early stage.

References

1. D.J. Lloyd, Particle Reinforced Aluminium and Magnesium Matrix Composites, *Int. Mater. Rev.*, Vol 39, 1994, p 1-23
2. J.D. Eshelby, *Proc. R. Soc., (London) A*, Vol 241, 1957, p 376
3. R.J. Arsenault and M. Taya, Thermal Residual Stress in Metal Matrix Composites, *Acta Metall.*, Vol 35, 1987, p 651-659
4. A. Levy and J.M. Papazian, Tensile Properties of Short Fiber-Reinforced SiC/Al Composites: Part II. Finite Element Analysis, *Metall. Trans. A*, Vol 21, 1990, p 411-420
5. A. Levy and J.M. Papazian, Thermal Cycling of Discontinuously Reinforced SiC/Al Composites, *Acta Metall.*, Vol 40, 1992, p 475-482
6. X.Q. Xu and D.F. Watt, Basic Role of a Hard Particle in a Metal Matrix Subjected to Tensile Loading, *Acta Metall.*, Vol 42, 1994, p 3717-3729
7. M.R. Wisnom, Factors Affecting the Transverse Tensile Strength of Unidirectional Continuous Silicon Carbide Fibre Reinforced 6061 Aluminium, *J. Comp. Mater.*, Vol 24, 1990, p 707-726
8. H. Sadouki and F.H. Wittmann, On the Analysis of the Failure Process in Composite Materials by Numerical Stimulation, *Mater. Sci. Eng., A* Vol 104, 1988, p 9-20
9. T. Christman, A. Needleman, and S. Suresh, An Experimental and Numerical Study of Deformation in Metal-Ceramic Composites, *Acta. Metall.*, Vol 37, 1989, p 3029-3050
10. S. Ho and A. Saigal, Three-Dimensional Modelling of Thermal Residual Stresses and Mechanical Behavior of Cast SiC/Al Particulate Composites, *Acta Metall. Mater.*, Vol 42, 1994, p 3253-3262
11. J. Llorca and P. Poza, Influence of Reinforcement Fracture on the Cyclic Stress-Strain Curve of Metal-Matrix Composites, *Acta. Metall. Mater.*, Vol 43, 1995, p 3959-3969
12. L.M. Wyatt (Ed.), *The Fulmer Materials Optimizer*, Fulmer Research Institute Limited, Berkshire (UK), Vol II, Part 3, 1974
13. S. Baragetti and M. Guagliano, On the Effect of Shot Peening on Fatigue Strength of Al/Al_2O_3 Composite Materials, *Proc. Mater. Eng.*, XXV AIAS National Conference, Gallipoli (LE), Sept 4-7 1996
14. *Abaqus Users' Manual*, Vol II, Version 5.5, HKS, Pawtucket (USA), 1995
15. Z.H. Zhong, *Finite Element Procedures for Contact-Impact Problems*, Oxford University Press, Oxford (UK), 1993, p 79-80